ISBN: 978-3-95450-132-8 doi:10.18429/JACoW-IPAC2014-TUPRO053

DESIGN AND OPTIMIZATION OF RACETRACK MICROTRON FOR LASER COMPTON SCATTERED GAMMA-RAY SOURCES

R. Hajima, M. Ferdows, JAEA, Tokai, Ibaraki, 3191195 Japan

Abstract

In the industrial application of laser Compton scattered gamma-ray sources for purposes of nuclear security, a racetrack microtron (RTM) with 220 MeV electron energy will be a suitable device to produce 1.7 MeV gamma-ray beams. Single electron bunch from a photocathode RF gun is accelerated and a high-charge small-emittance beam is preferable in such RTM. In this paper, we adopt a simulation code, GPT, for design and optimization of a 220-MeV RTM.

INTRODUCTION

Non-destructive inspection for screening special nuclear materials (SNM) at port-of-entries is of growing importance in view of the nuclear security, which is the detonation by terrorists of a yield-producing nuclear bomb containing fissile material such as ^{235}U or ^{239}Pu with the weights of several kilograms. We have proposed a SNM inspection system, which is a hybrid system of two different probes, neutrons and γ-rays [1]. In this system, a cargo is irradiated with laser Compton scattered γ-rays to identify the isotope composition of the materials by using nuclear resonance fluorescence (NRF) [2].

For developing the proposed SNM inspection system, we are conducting experimental studies utilizing an existing 150-MeV racetrack microtron (RTM) at JAEA, where generation of LCS γ-ray of 400 keV and nondestructive detection of specific isotope are carried out [3].

In parallel with the experimental studies, design of a 220-MeV RTM has been elaborated for our SNM inspection system in a future practical use. The energy of 220 MeV was chosen because the detection of ^{235}U requires 1.7 MeV γ-ray beams, which can be generated from a collision of 220 MeV electrons and a frequency-doubled Nd:YAG laser. So far, the design study has been made with a particle tracking code, MIC, particularly developed for a racetrack microtron [4]. In this paper, we present a design of 220-MeV RTM with GPT (General Particle Tracer) [5] as complementary to MIC simulations.

MODELING A 220-MeV RACETRACK MICROTRON

The 220-MeV RTM for the SNM detection is equipped with a photocathode RF gun as an injector. This configuration is same as our 150-MeV RTM [6]. Using a photocathode RF gun, we can inject an electron bunch short enough to match a small longitudinal acceptance of RTM. Injection of a single electron bunch with relatively large charge is also preferable for a high-flux LCS γ-ray generation with a commercially available Nd:YAG laser.

A simulation model presented here, however, does not include the injector. The model is similar to our previous study [4] and we assume a RTM consisting of a 0.5m-long S-band linac, a pair of main dipole magnets (1.48 T) and thin reverse bend magnets located at the entrance of the main dipoles. A 3-dimensional field map of the main dipole is generated by a separate program and GPT reads the map file. The reverse bend is implemented as a rectangular magnet with fringe field defined in GPT. There are no quadrupole magnets for transverse focusing and chicane magnets for injection and extraction. Transverse focusing along the recirculation is established by field gradient of the main dipole and reverse bend magnets. Additional transverse focusing is obtained by linac, which is a side-coupled standing wave structure.

All the simulation is initiated with an electron bunch at the entrance of linac. The injection electron energy is chosen to be about 7 MeV to eliminate a U-turn orbit at the first pass.

Figure 1 and 2 are field profiles of unit cell and whole structure of the standing wave linac of side-coupled cavity type calculated by SUPERFISH.

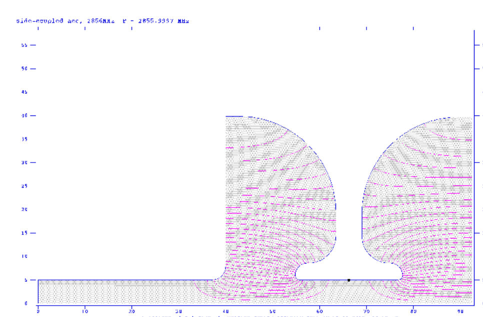

Figure 1: Cavity shape and accelerating field profile of the standing wave linac used in our model.

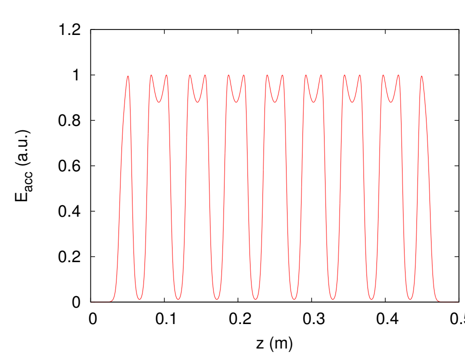

Figure 2: Field profile of the standing wave linac.

Content from this work may be used under the terms of the CC BY 3.0 licence (© 2014). Any distribution of this work must maintain attribution to the author(s), title of the work, publisher, and DOI.

ISBN: 978-3-95450-132-8 doi:10.18429/JACoW-IPAC2014-TUPRO053

Figure 3 shows an example of electron orbit calculated by GPT, where the linac is located at $0 < z < 0.5$ m. From the resonance condition of RTM

$$\Delta E(\mathrm{MeV}) = \frac{\nu\lambda(\mathrm{cm})}{2.096} B(\mathrm{T}) \tag{1}$$

and $\nu = 1$, $\lambda = 10.5$ cm, $B = 1.48$ T, we have energy gain per pass to be 7.4 MeV. After 28 recirculations, electron beam energy exceeds 220 MeV.

It should be noted that GPT simulations are conducted in the global coordinate, while electron motion is tracked along a local coordinate of curved trajectory in PARMELA and ELEGANT. Thus, multi-pass acceleration of electrons with longitudinal and transverse phase space motion becomes self-consistent in GPT simulations. A dipole magnet with canted poles specific to RTM can be dealt with GPT.

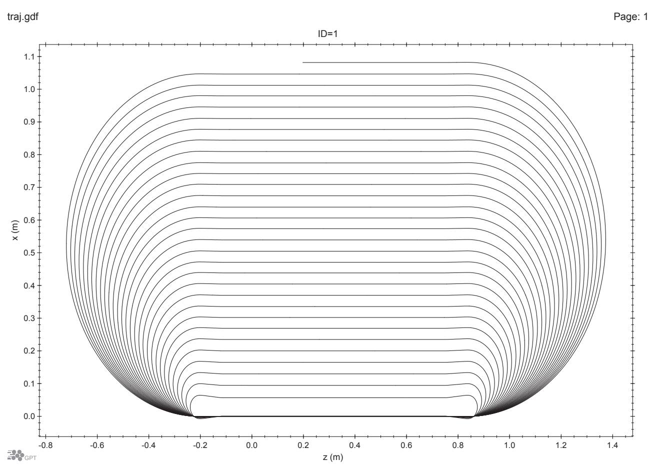

Figure 3: Electron orbit calculated by GPT.

LONGITUDINAL MOTION

In the design of 220-MeV RTM, we have several parameters to be optimized, which are loop length, field of main dipole and reverse bend, voltage and phase of linac. In our design simulations, we employ a wrapper script written in Perl to create a GPT input with scanning the above parameters in a systematic manner [7]. The parameters have been optimized to obtain large acceptance both in longitudinal and transverse phase spaces. After the parameter optimization, we found a design to accelerate electrons from the initial kinetic energy of 7.8 MeV to the final energy of 230.1 MeV after 31 passes as shown in Fig. 3. The number of passes to exceed 220 MeV is larger than expected from Eq.(1), because the main dipole magnets have a field gradient as seen in the next section.

In order to evaluate the acceptance of RTM, we put three collimators to reject electrons deviated from the design orbit. Two collimators are located at the entrance and exit of linac and have rectangular apertures, 1 cm × 1 cm, and the third slit is located at $z = 0$ to restrict a vertical aperture to 1 cm. The third slit does not interfere electrons passing the linac, because the slit is defined in a custom coordinate system (CCS), in which electrons travel to the left direction in Fig. 3.

Figure 4 is a longitudinal acceptance of the designed RTM, where final energy of electrons are plotted as a function of initial energy and longitudinal position. We can see that the phase acceptance is only 5 mm (~ 16 *ps*) even after the optimization. The acceptance is not so large but we consider it is adequate for injection from a photocathode RF gun.

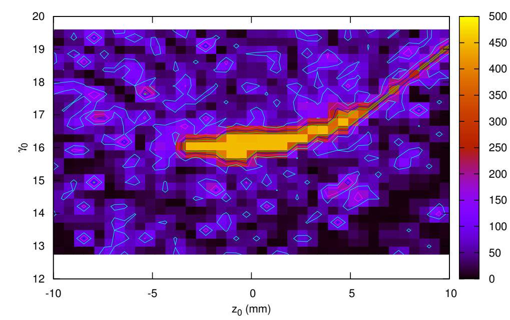

Figure 4: Longitudinal acceptance for initial kinetic energy 7.8 MeV. The contour colors represent final energy of electrons (γ).

TRANSVERSE MOTION

In the 220-MeV RTM, field gradient of the main dipole and the reverse bend are the tuning parameters for the optimization of transverse acceptance. In our simulations, we have fixed the main dipole field and varied the reverse field to enlarge the transverse acceptance.

Figure 5 shows magnetic field profile along z-axis. The main dipole field decreases linearly along z-axis with a gradient of $dB_y/dz = -0.14$ T/m. We found that reverse bend of $B = -0.53$ T shows the largest transverse acceptance in our model. Figures 6 shows beam envelopes in the horizontal and vertical planes for two different values of reverse bend, -0.5 T and -0.53 T. In the envelope simulation, we assume the initial beam size as small as 5 mm × 5 mm so that all the particles survive to the end. It can be seen in Fig.7 that the beam is tightly focused in the vertical plane with the reverse bend field of $-0,53$ T. The horizontal envelope, however, is not affected so much by changing the reverse bend field. This result suggests that the horizontal focusing is mainly obtained by standing wave linac.

After the optimization of reverse bend field, we estimate the transverse acceptance. Transverse acceptance for the horizontal and vertical planes is plotted in Fig. 7, where contour is the particle energy (γ) after acceleration to the end or collimated by finite aperture during acceleration. The transverse acceptance is roughly estimated at $7 - 8\pi$ mm-mrad in both horizontal and vertical phase spaces at the kinetic energy of 7.8 MeV, which corresponds to normalized acceptance of $110 - 120\pi$ mm-mrad.

Content from this work may be used under the terms of the CC BY 3.0 licence (© 2014). Any distribution of this work must maintain attribution to the author(s), title of the work, publisher, and DOI.

ISBN: 978-3-95450-132-8 doi:10.18429/JACoW-IPAC2014-TUPRO053

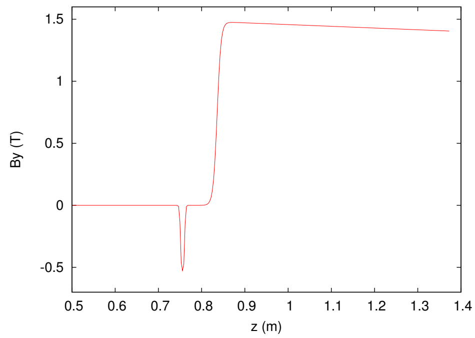

Figure 5: Magnetic field profile along z-axis. The edge of main dipole is located at $z = 0.836$ m.

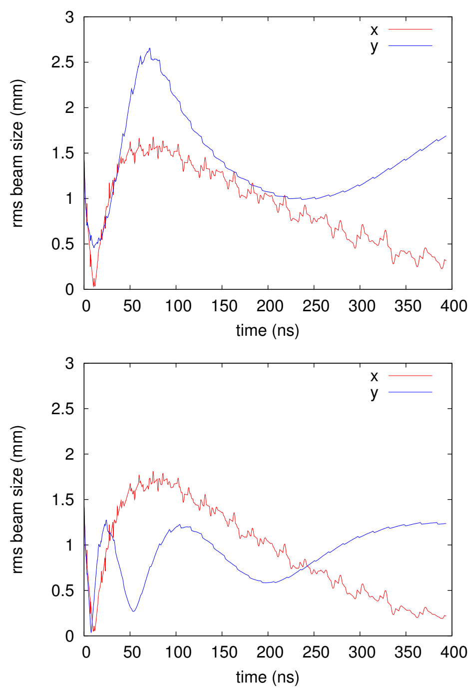

Figure 6: Electron beam envelope in the horizontal plane (x) and vertical plane (y) calculated for reverse bend field of −0.5 (top) and −0.53 T (bottom).

CONCLUSION

Design of a 220-MeV RTM has been carried out with a particle tracking code, GPT. The feature of GPT, particle tracking in the global coordinate with arbitrary magnetic field, allows us to make a self-consistent simulation of RTM. Design optimization for large acceptance in longitudinal and transverse phase spaces has been conducted by tuning the geometry of accelerator component, accelerator voltage and profile of magnetic field. Simulations including an RF injector, chicanes for injection and extraction, collective force due to space charge and coherent radiation will be done in the near future. Reduction of injection energy is another issue remains to be discussed.

This work is supported by Funds for Integrated Promotion of Social System Reform and Research and Development. The authors are grateful to T. Hori and F. Sakai for discussion about RTM. The authors would like to thank T. Miyajima at KEK who gave helpful advice on GPT simulations.

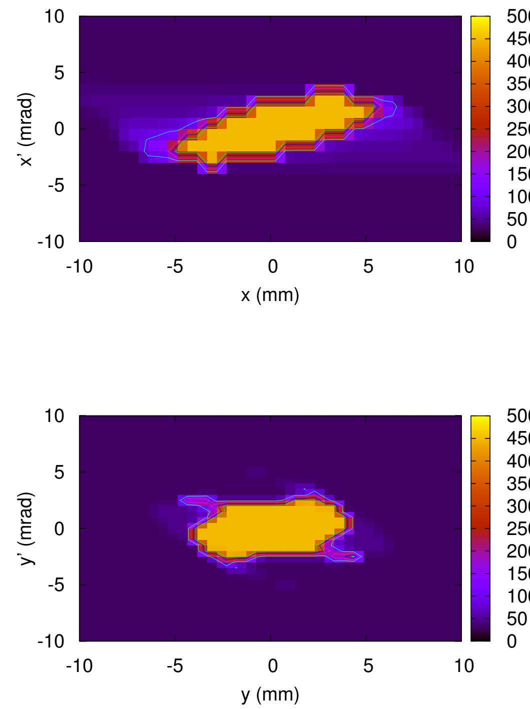

Figure 7: Transverse acceptance of the horizontal and vertical phase spaces calculated for reverse bend field of −0.53 T. The contour colors represent final energy of electrons (γ).

REFERENCES

[1] H. Ohgaki et al. J. Korean Phys. Soc., **59**, 31553159 (2011).

[2] R. Hajima et al., J. Nucl. Sci. Tech. **45**, 441 (2008).

[3] R. Hajima et al., Proc. IPAC-2013, 3645 (2013).

[4] T. Hori et al., Proc. IPAC-2013, 3651 (2013).

[5] General Particle Tracer, Pulsar Physics.

[6] M. Kando et al., Proc. PAC-1999, 3702 (1999).

[7] R. Hajima and R. Nagai, Nucl. Inst. Meth. **A557**, 103 (2006).

Content from this work may be used under the terms of the CC BY 3.0 licence (© 2014). Any distribution of this work must maintain attribution to the author(s), title of the work, publisher, and DOI.